Insight into an unusual lanthanum effect on the oxygen reduction reaction activity of Ruddlesden-Popper-type cation-nonstoichiometric $La_{2-x}NiO_{4+\delta}$ (x=0~0.1) oxides

Yubo Chen,[a] Baoming Qian,[a] Guangming Yang,[a] Dengjie Chen[b] and Zongping Shao[a,c]

[a] *State Key Laboratory of Materials-Oriented Chemical Engineering, College of Chemistry & Chemical Engineering, Nanjing Tech University, Nanjing 210009, China*

[b] *Department of Mechanical and Aerospace Engineering, The Hong Kong University of Science and Technology, Hong Kong, SAR China.*

[c] *College of Energy, Nanjing Tech University, Nanjing 210009, China*

Table S1 The interplanar spaces measured from the diffraction data and the values calculated from the Rietveld refinement of X-ray diffraction.

zone axis	[001]		[121]				[141]		
	(20)	(20)	(00)	(11)	(04)	(3)	(13)	(5)	(02)
Mea.(Å)*	2.70	1.92	2.75	3.65	2.04	2.78	2.82	2.12	2.49
Cal.(Å)**	2.69	1.91	2.71	3.70	2.07	2.85	2.85	2.12	2.51

* Measured interplanar spaces from the diffraction data.

** Calculated from the Rietveld refinement of X-ray diffractions.

Table S2 The fitting data of the La-deficient $La_{2-x}NiO_{4+\delta}$ samples.

	Temperature(°C)	750	700	650	600	550	500
$La_{1.98}NiO_{4+\delta}$							
Arc1	R1 (Ω cm^2)	/	/	/	0.595	1.402	3.6109
	C1 (F cm^{-2})	/	/	/	1.511E-9	1.2266E-9	3.289E-9
	f1 (Hz)	/	/	/	1.772E8	9.263E7	1.341E7
Arc2	R2 (Ω cm^2)	0.3208	0.6384	1.4834	4.609	11.211	31.922
	C2 (F cm^{-2})	4.798E-5	2.654E-5	2.446E-5	4.29E-5	3.138E-5	2.346E-5
	f2 (Hz)	10346.3	9396.9	4388.3	805.3	452.6	212.62
Arc3	R3 (Ω cm^2)	0.423	0.9323	2.153	4.5407	13.567	46.80
	C3 (F cm^{-2})	0.001893	0.00183	0.002139	0.004706	0.004675	0.00494
	f3 (Hz)	198.79	93.29	34.576	7.4528	2.5106	0.6886
$La_{1.95}NiO_{4+\delta}$							
Arc1	R1 (Ω cm^2)	/	/	/	0.5492	1.649	4.563
	C1 (F cm^{-2})	/	/	/	5.587E-8	4.802E-9	5.681E-9
	f1 (Hz)	/	/	/	5.190E6	2.011E7	6.143E6

Arc2	R2 (Ω cm^2)	0.5823	0.7398	2.817	7.506	20.528	44.59
	C2 (F cm^{-2})	3.406E-5	1.133E-5	1.619E-5	1.812E-5	1.619E-5	9.14E-5
	f2 (Hz)	8029.5	19000.4	3491.1	1170.8	479.1	390.66
Arc3	R3 (Ω cm^2)	0.42051	1.443	2.1991	4.861	13.136	60.74
	C3 (F cm^{-2})	0.00246	0.000807	0.003078	0.00591	0.00846	0.004765
	f3 (Hz)	153.7	136.77	23.53	5.54	1.432	0.5502
$La_{1.90}NiO_{4+\delta}$							
Arc1	R1 (Ω cm^2)	/	/	/	0.6327	1.90014	5.0037
	C1 (F cm^{-2})	/	/	/	1.913E-8	3.0379E-9	3.929E-9
	f1 (Hz)	/	/	/	1.316E7	2.759E7	8.101E6
Arc2	R2 (Ω cm^2)	0.7689	1.05268	3.0865	9.197	21.95	44.964
	C2 (F cm^{-2})	2.844E-5	1.209E-5	1.591E-5	2.004E-5	1.4839E-5	1.176E-5
	f2 (Hz)	7282.3	12505.56	3243.3	864.22	489.00	301.2
Arc3	R3 (Ω cm^2)	0.2809	1.2357	2.252	3.795	15.353	63.781
	C3 (F cm^{-2})	0.005022	0.00102	0.002503	0.007577	0.005788	0.003435
	f3 (Hz)	112.887	126.3	28.252	5.5386	1.7921	0.7269

Table S3 the fitting parameters of $La_2NiO_{4+\delta}$ at different oxygen partial pressures (0.05~0.4atm).

P_{O2} (atm)			0.05	0.1	0.2	0.4
550 °C	Arc1	R1 (Ω cm^2)	1.768	1.768	1.768	1.768
		C1 (F cm^{-2})	1.089E-10	7.40E-11	8.383E-11	1.113E-10
		f1 (Hz)	796408674	1171489589	1034262424	964402905
	Arc2	R2 (Ω cm^2)	12.462	11.4801	9.803	10.623
		C2 (F cm^{-2})	4.729E-5	4.520E-5	4.949E-5	1.859E-5
		f2 (Hz)	260.11	295.4	315.94	806.0
	Arc3	R3 (Ω cm^2)	24.24	16.735	11.97	13.26
		C3 (F cm^{-2})	0.004858	0.00536	0.005788	0.00757

		f3 (Hz)	1.3017	1.7075	2.213	1.585
600 ºC	Arc1	R1 (Ω cm²)	5.328	4.358	3.678	2.8173
		C1 (F cm⁻²)	5.544E-5	5.640E-5	3.9696E-5	5.425E-5
		f1 (Hz)	518.99	623.62	1050.04	1002.87
	Arc2	R2 (Ω cm²)	8.596	6.231	4.513	3.4611
		C2 (F cm⁻²)	0.00484	0.00475	0.00452	0.00428
		f2 (Hz)	3.682	5.182	7.507	10.347
650 ºC	Arc1	R1 (Ω cm²)	2.376	1.7217	1.476	1.1584
		C1 (F cm⁻²)	5.989E-5	7.476E-5	6.37E-5	6.029E-5
		f1 (Hz)	1077.2	1190.85	1630.89	2194.7
	Arc2	R2 (Ω cm²)	3.3537	2.594	1.828	1.373
		C2 (F cm⁻²)	0.005033	0.003803	0.00387	0.00378
		f2 (Hz)	9.0817	15.537	21.679	29.517
700 ºC	Arc1	R1 (Ω cm²)	0.9182	0.729	0.515	0.463
		C1 (F cm⁻²)	8.49E-5	8.65E-5	7.0987E-5	8.493E-5
		f1 (Hz)	1966.187	2431.77	4194.8	3898.4
	Arc2	R2 (Ω cm²)	1.5571	1.127	0.897	0.6152
		C2 (F cm⁻²)	0.00384	0.003396	0.00247	0.00293
		f2 (Hz)	25.62	40.042	69.056	84.943
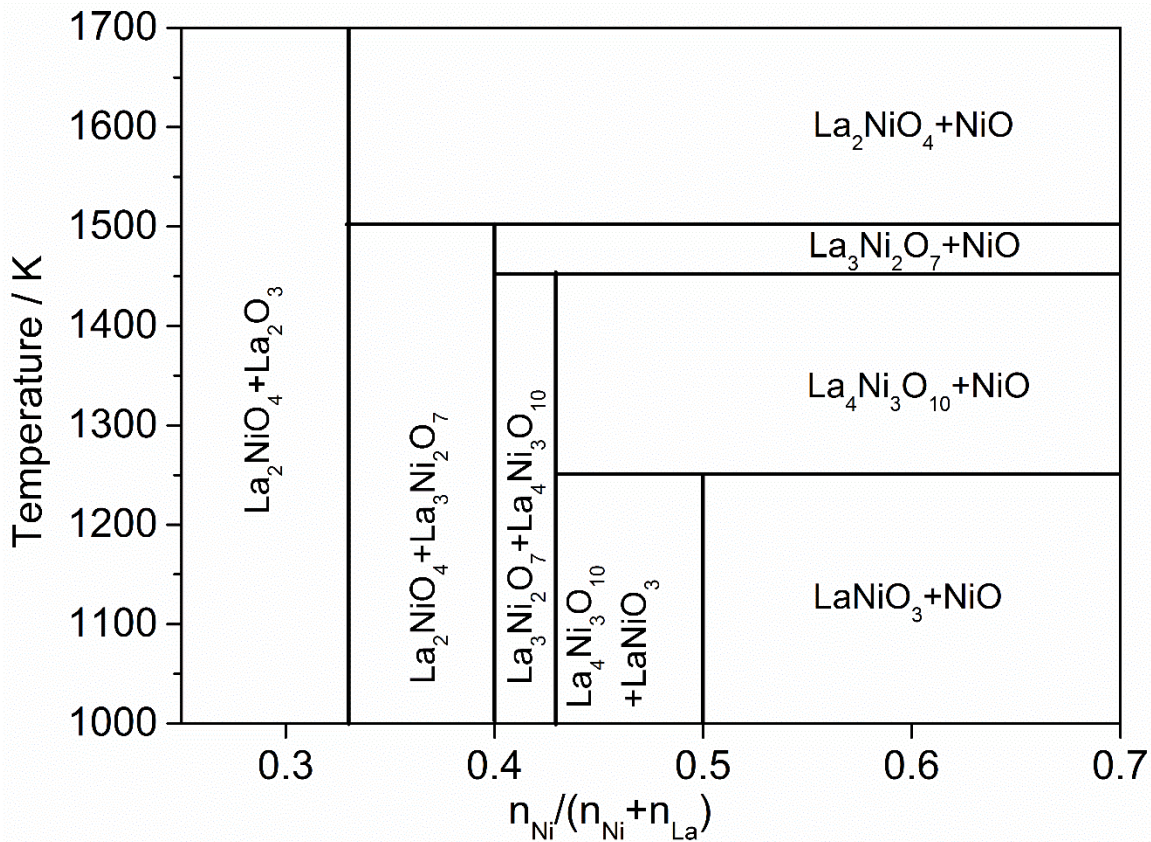
**Figure S1** A thermodynamic calculation of stable phase composition of the ternary La–Ni–O system.
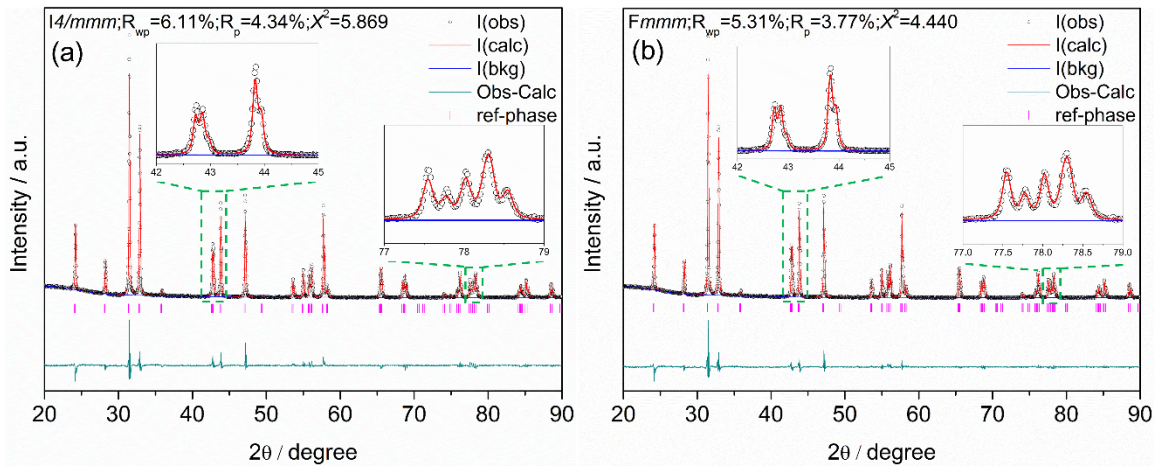
Figure S2 Refined diffraction patterns of $La_2NiO_{4+\delta}$ phase.
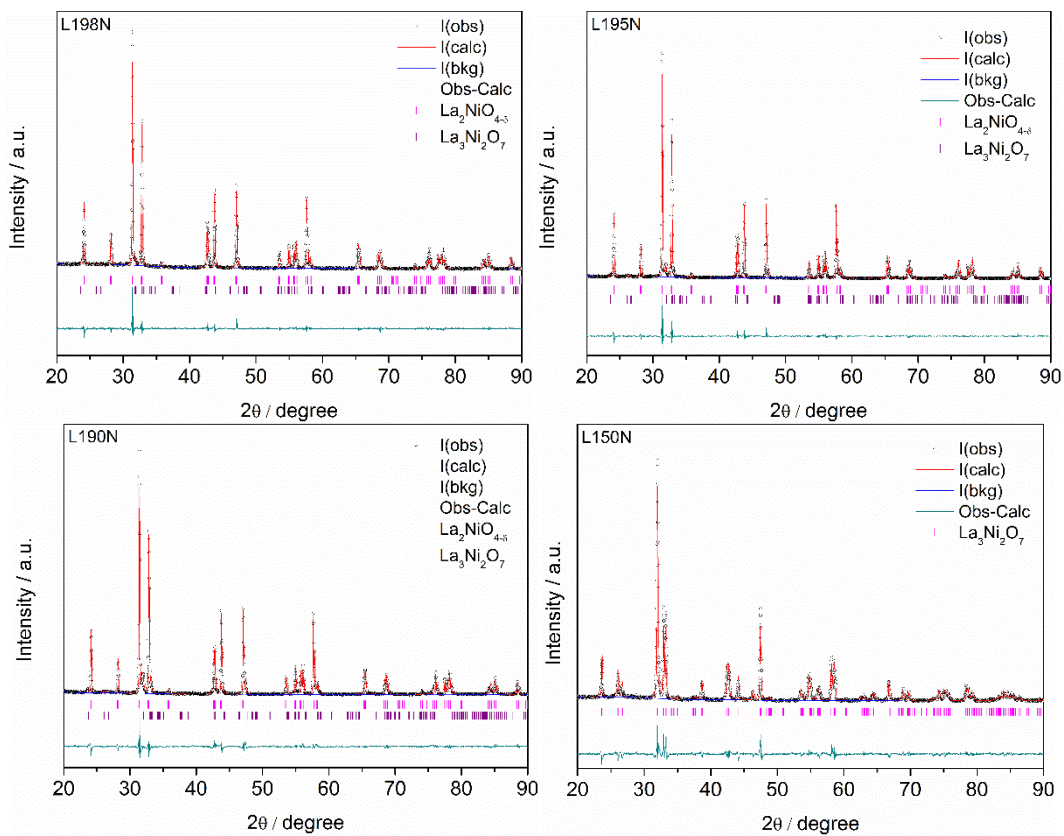
**Figure S3** The refined diffraction patterns of the La-deficient $La_{2-x}NiO_{4+\delta}$ phases.
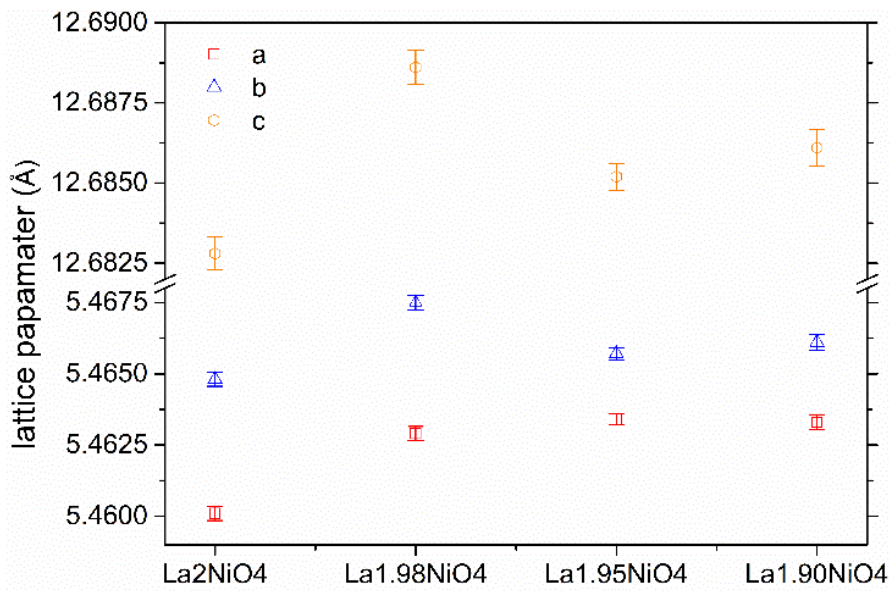
**Figure S4** Variation of lattice parameters (a, b and c) of primary $La_2NiO_{4+\delta}$ phase in samples.
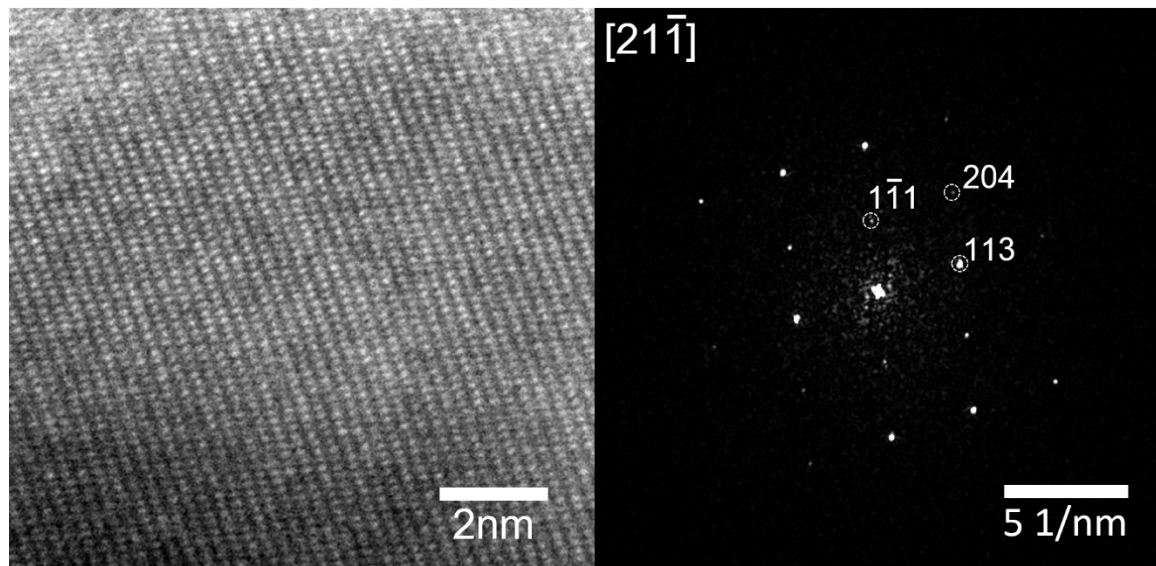
Figure S5 HRTEM image of a $La_{2-x}NiO_{4+\delta}$ sample (a) and the corresponding diffraction patterns acquired via FFT (b).
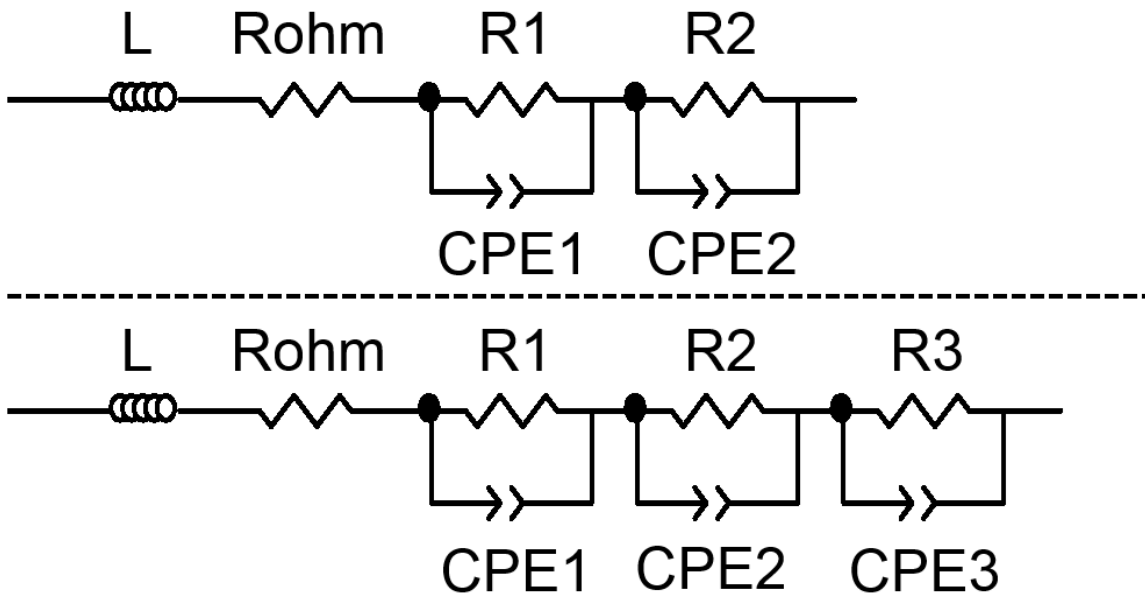
**Figure S6** The equivalent circuit of the type L-Ro-(R1‖CPE1)-(R2‖CPE2)-…-(Ri‖CPEi).
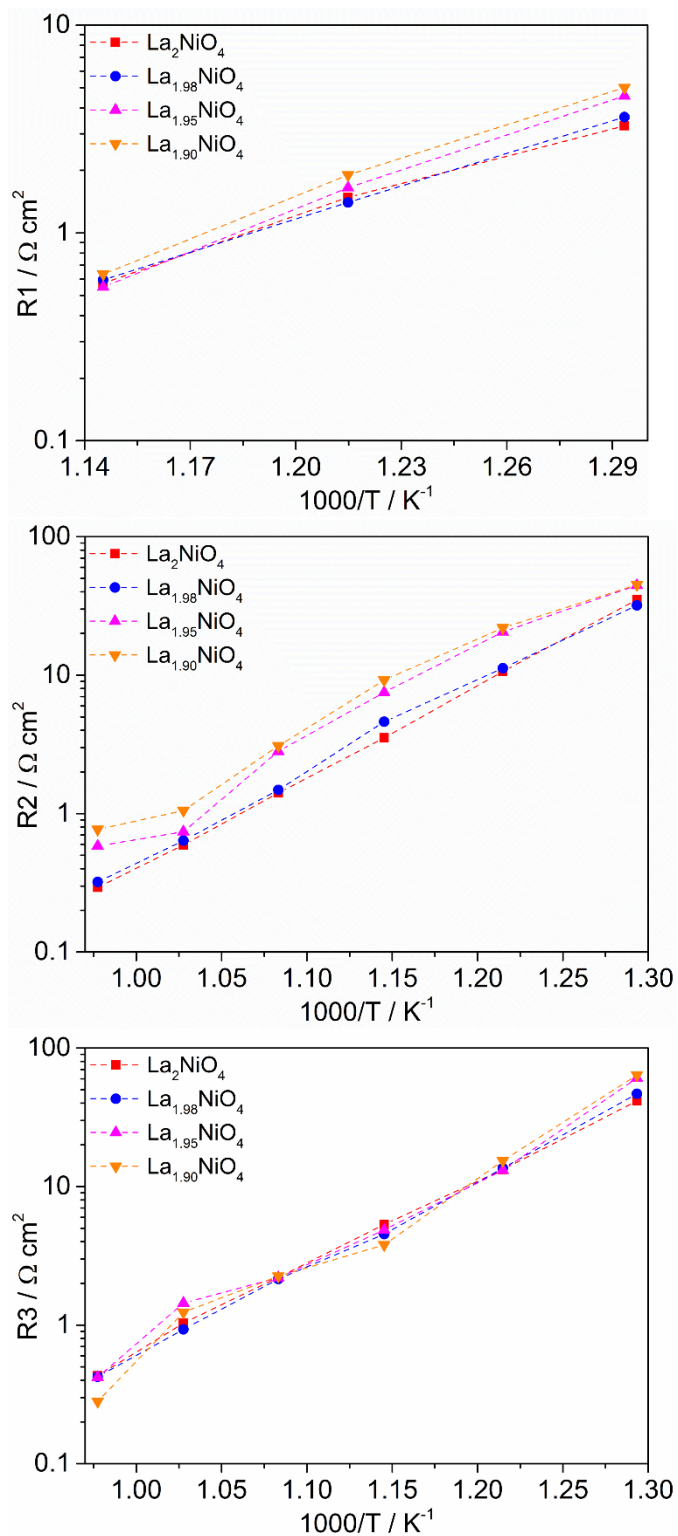
Figure S7 The resistances belonging to three arcs from the spectra at high (R1), medium (R2) and low (R3) frequency.
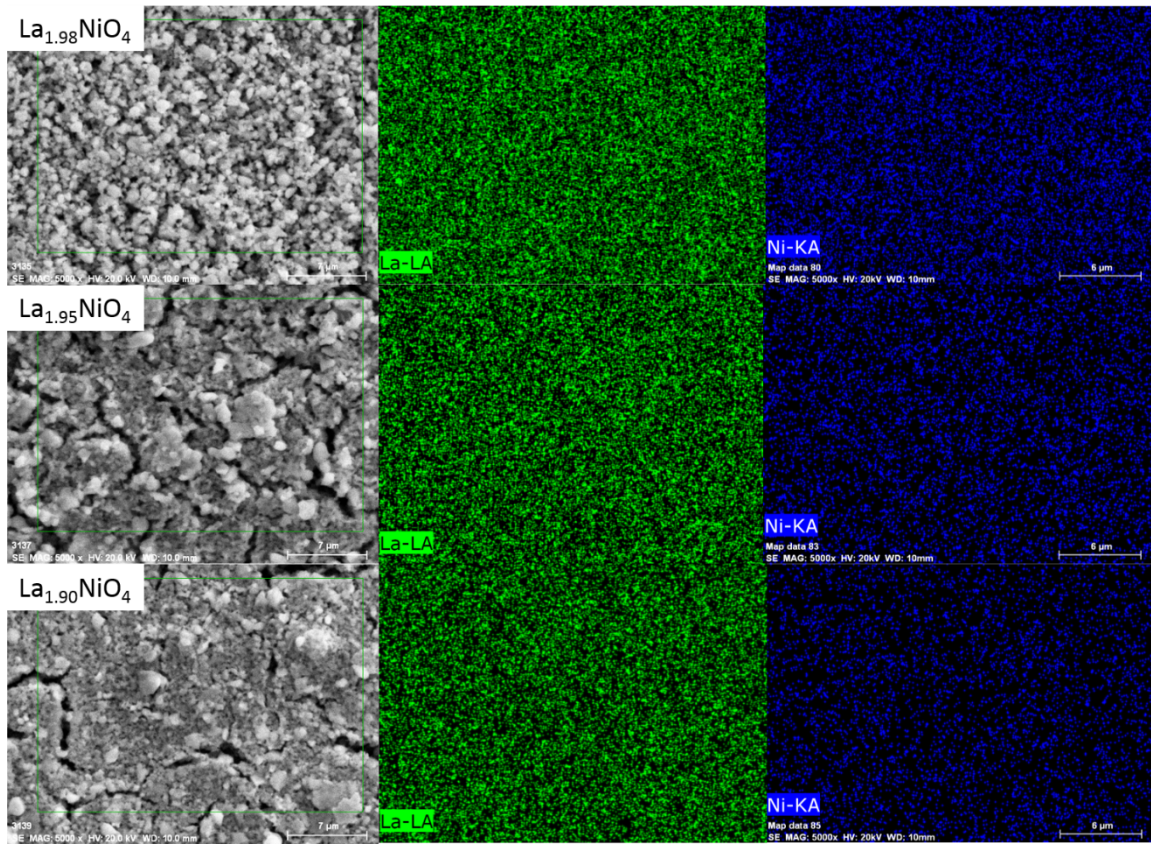
Figure S8 Situations of elemental distribution of three La-deficient electrodes.
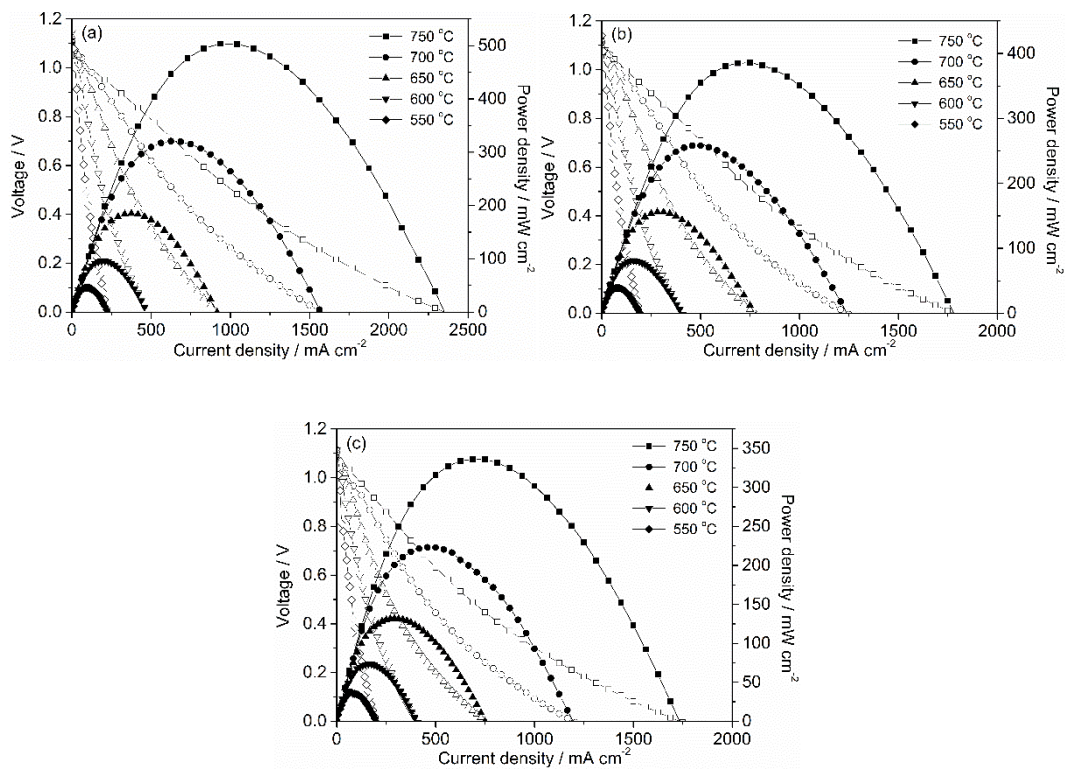
Figure S9 the *I-V* curves of fuel cells with $La_{2-x}NiO_{4+\delta}$ materials as cathodes.